SEMARAK ILMU PUBLISHING

Journal of XX

Journal homepage:
https://semarakilmu.com.my/journals/
ISSN: XXXX-XXXX

# A Parametric Study of Small-Scale Offshore Vertical Axis Wind Turbines: Unlocking Potential in Low Wind Profile Regions

Norzaima Nordin[1,*], Nur Ezalifah Ahmad Mokhtar[2], Maidiana Othman[3], Muhamad Nur Alif Nadzri[2], Mohd Rashdan Saad[1], Mohamed Tarmizi Ahmad[1]

[1] Department of Aeronautical Engineering and Aviation, Faculty of Engineering, Universiti Pertahanan Nasional Malaysia, 57000, Sungai Besi, Kuala Lumpur, Malaysia
[2] Department of Mechanical Engineering, Faculty of Engineering, Universiti Pertahanan Nasional Malaysia, 57000, Sungai Besi, Kuala Lumpur, Malaysia
[3] Department of Civil Engineering, Faculty of Engineering, Universiti Pertahanan Nasional Malaysia, 57000, Sungai Besi, Kuala Lumpur, Malaysia

**ARTICLE INFO**

***Article history:***
Received 29 October XXXX
Received in revised form 1 December XXXX
Accepted 9 December XXXX
Available online 10 December XXXX

***Keywords:***
Low wind speed; Offshore; Power coefficient, Taguchi method; Tip speed ratio; Vertical axis wind turbine

**ABSTRACT**

In recent decades, wind turbines have emerged as substantial renewable energy technology, particularly for offshore applications. However, the utilisation of conventional wind turbine in regions characterised by a low wind speed profiles, such as Malaysia, remains limited. Therefore, this study addresses the gap by developing an unconventional small-scale Vertical Axis Wind Turbine (VAWT) provision for offshore application in Malaysia's low wind speed regions. The study commenced with a wind feasibility analysis which aimed to determine the viable range of offshore wind speeds prior conducting wind tunnel tests. The VAWT model was designed using Solidworks software, fabricated using a 3D printer and tested in the National Defence University of Malaysia (UPNM) wind tunnel lab facilities. Through a systematic analysis and optimisation of blade diameters, stages and angles using Taguchi method, this study aimed to enhance the wind turbine performance in terms of power coefficient ($C_p$) and tip speed ratio. The result highlighted the pivotal role of blade diameter and the number of stages as a key design factors for VAWT, with the optimal configuration of blade diameter of 16 cm, a single stage and Angle of Attack (AoA) set at 7°. This configuration exhibited a remarkable $C_p$ value of 0.622, signifying the power output efficiency of small-scale VAWT. Meanwhile, variations in AoA were found to be the least significant design factor, as all models demonstrated peak $C_p$ values corresponding to wind speeds. Thus, these findings show the key design considerations for small-scale VAWT in low wind profile regions as well as contributing valuable knowledge for the sustainable development of wind energy in Malaysia.

## 1. Introduction

A wind turbine is a renewable energy technology that converts wind energy into electricity through the aerodynamic force generated by its rotor blade. As the wind flows across the blades, a drop in air pressure on one side creates lift and drag, establishing a differential air pressure over the blade surfaces. This phenomenon generates a lift force surpassing the drag force, causing the rotor blade to spin. The blade is directly connected to the generator, either through a direct drive from the

* *Corresponding author.*
*E-mail address: norzaima@upnm.edu.my (Norzaima Nordin)*

turbine or through a shaft and series of gears (gearbox). This conversion of aerodynamic force to rotational motion in the generator produces the power output of the turbine. There are two main types of wind turbines: Horizontal Axis Wind Turbine (HAWT) and Vertical Axis Wind Turbine (VAWT). The part diagrams for HAWT and VAWT are illustrated in Figure 1. HAWTs are the most commonly used turbines due to their strength and efficiency. In HAWT systems, the entire rotor, gearbox and generator are located at the top of the tower and must be oriented to face the wind direction. Khillar [1] noted that, in contrast, VAWT is omnidirectional, allowing the rotor to capture wind from any direction. As a result, there is no need for a yaw mechanism in VAWT and it does not require constant adjustment or exposure to high-velocity winds.

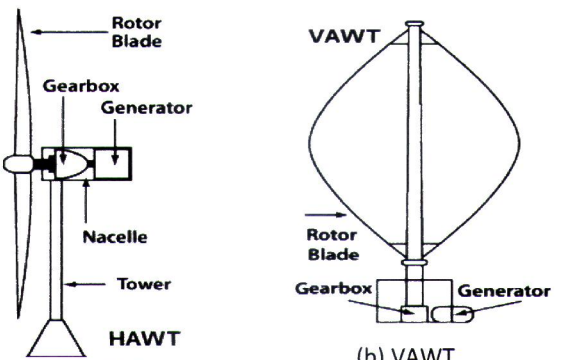


(a) HAWT (b) VAWT

**Fig. 1.** Parts diagram of wind turbine [2]

VAWTs are generally categorises into two types: drag type and lift type. The Savonius turbine is a drag-type category, boasting higher torque capabilities while requiring less wind energy input. Meanwhile, Darrieus turbine characterised as a lift-type design wherein the aerodynamic of the airfoil generate a lift force. A notable advantage of VAWTs is the design relative ease of maintenance compared to HAWTs. Óskarsdóttir [3] highlighted additional benefits including the ability of crossflow devices to capture wind from any direction, negating the need for the costly yaw drive gear present in HAWTs. To address low-speed conditions, a desirable feature is the integration of a mixed Darrieus-Savonius wind turbine. The Savonius rotor serves as a starting mechanism, aiding the turbine in low wind speeds and assisting in driving the Darrieus rotor. Jamanun *et al.,* [4] noted that the Darrieus-Savonius mixed turbine demonstrate superior power generation and self-start capabilities in low wind speed conditions. By merging these two blades type onto a single rotor has the potential to mitigate the drawbacks inherent in each type. Hence, a mixed VAWT was chosen in this study, showcasing remarkable advantages that make it well-suited for optimal performance, particularly in regions characterised by low wind speed, such as the coastal areas of Malaysia.

Malaysia, situated in Southeast Asia at 2°30'N latitude and 112°30'E, is characterised by its unique geographical location where it experiences two distinct monsoon seasons. With the Northeast monsoon prevailing from November to March and the Southwest monsoon from May to September, the country faces challenges in wind energy development due to consistently low wind speeds, especially when compared to other nations. As noted by Mekhilef *et al.*, [5], offshore wind speed tends to be higher than onshore, contributing significantly to electricity generation. Previous research indicates that daily average wind speeds in Malaysia are nearly twice as high, at 2 m/s, compared to early morning and night speed, which average at 1 m/s [6]. Similar prediction found by Hashim *et al.,* [7] where the Malaysia's annual offshore wind speed to range between 1.2 m/s and 4.1 m/s, with in eastern Peninsular Malaysia experiencing values from 3.3 m/s to 4.1 m/s. During the northeast monsoon season, Malaysia's coastline experienced wind speed exceeding 5 m/s. This data

suggested the potential wind speeds for offshore application ranging from 5 m/s to 9 m/s. Despite early attempts at wind energy implementations in locations like Terumbu Layang-Layang, Sabah and Perhentian Island, Terengganu, initial finding showed insufficient wind and functionality issues, with certain project remaining under-proposed [8]. In the prior investigation conducted by Albani *et al.* [9], there are nine (9) potential prospective locations identified for the study and implementing offshore wind turbines shown in Figure 2 and Table 1.

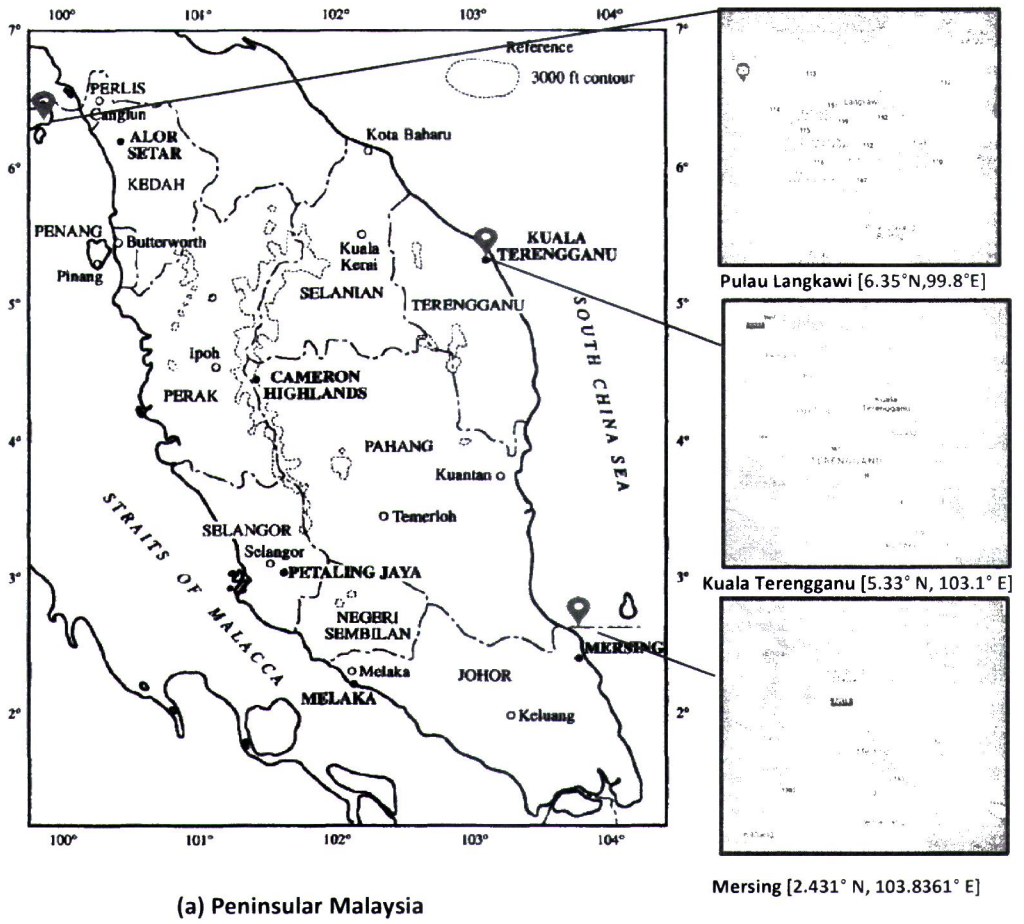


**Fig. 2.** Nine (9) potential offshore stations in Malaysia

**Table 1**
Potential Offshore Locations in Malaysia

| Locations | Latitude °N | Longitude °E | Height above Sea Level (m) |
|---|---|---|---|
| Pulau Langkawi | 6.35° | 99.8° | 6.4 |
| Kuala Terengganu | 5.33° | 103.1° | 5.2 |
| Mersing | 2.431° | 103.83° | 43.6 |
| Kuching | 1.553° | 110.359° | 21.7 |
| Bintulu | 3.174° | 113.043° | 23.1 |
| Tawau | 4.245° | 117.891° | 17.0 |
| Kota Kinabalu | 5.980° | 116.074° | 2.3 |
| Sandakan | 5.84° | 118.12° | 10.3 |
| Kudat | 6.883° | 116.85° | 3.5 |

These strategically selected locations, each characterised by unique geographic and elevation features, served as vital reference points for the wind speed analysis in the present study. The Renewable Ninja Tool was employed to conduct an extensive analysis of wind patterns at these nine (9) locations, underscoring the importance of considering geographic and elevation characteristic in assessing wind potential for energy generation.

Most of the wind turbine models developed in Malaysia utilise the HAWT design [10-12]. Given Malaysia's low wind speed region, the design of wind turbine employing VAWT become more feasible especially for low wind profile regions. It is crucial to note that the parameters of wind turbine blades significantly impact their performance. The efficiency of a VAWT can be assessed based on factors such as its turbine type and blade design. Integrating both Savonius and Darrieus blade types on a single turbine offers improvements to the drawbacks of each type [13]. Blade diameter, the number of stages and the angle of attack (AoA) are key parameters in determining wind turbine performance [14-15]. Increasing these parameters enhances wind turbine performance, as well as the power coefficient ($C_p$) and tip speed ratio (TSR) of wind turbine.

Hence, this paper presents the potential design of a small-scale offshore wind turbine contributing to optimal power generation, particularly suitable for low wind speed offshore regions. The information provided guides the process of configuring and fabricating the Mixed VAWT, incorporating the selected parameters mentioned earlier. The Taguchi method, chosen for experimentation optimisation, will be employed in this study. The Taguchi experimental design minimizes costs, improves quality, as well as provides stable and reliable design solutions [16-21]. This method allows the simultaneous optimisation of numerous factors, extracting more quantitative information from fewer experimental trials compared to other methods.

## 2. Methodology

### *2.1 Base concept of Mixed VAWT*

Various enhancements have been introduced to optimise the performance of each blade type. Previous studies investigating the Savonius wind turbine's efficiency explored the impact of different parameters, such as the number of stages, overlap ratio, the number of blades and the use of end plates. Al-Ghriybah *et al.,* [22] demonstrated that the Darrieus rotor surpasses the Savonius rotor in terms of efficiency. The Savonius rotor exhibits advantageous features over the Darrieus rotor, including self-start capability, high starting torque, low maintenance costs and reduced noise. Zemamou *et al.*, [23] reported a maximum efficiency of 31% for the Savonius rotor, with a prototype achieving an efficiency of 37%. The combination of Savonius and Darrieus rotors yields superior performance at low wind speeds. The research methodology involves the development of a new

rotor structure and adjustment of blade parameters. Loganathan *et al.,* [24] observed a 50% increase in power output when the blade diameter was increased by 50%, demonstrating the direct relationship between diameter and energy capture. Previous experimental and numerical research, focusing on modifying a Savonius turbine with multiple stages, revealed that the coefficient of power ($C_p$) and coefficient of torque ($C_t$) increase with the number of stages. A two-stage rotor is chosen for this design, considering the advantages of reducing moment fluctuations, particularly in two-bladed rotors. Kadam and Patil [25] demonstrated that a two-blade rotor generates more mechanical power compared to three and four-blade rotors. The Darrieus type undergoes analysis regarding its angle of attack, suggesting potential improvements in performance by tilting the blade at specific angles. Prince *et al.,* [26] reported that low angles of Darrieus blades ($\alpha < 15°$) exhibit higher efficiency at lower velocity ratios ($\lambda < 0.1$) than higher blade angles. The turbine was found to be more efficient for $\lambda < 0.11$ with blade angles less than this value.

### *2.1.1 Swept Area ($A_s$)*

The swept area ($A_s$) serves as a characterisation metric for each Savonius wind turbine as illustrated in Figure 3. The size of the Savonius turbine blade significantly influences the energy output of the turbine. A larger surface area results in the collection of more energy. The swept area of the Savonius VAWT can be mathematically calculated using the rotor dimensions where $H$ and $D$ represent the height and diameter of rotor, respectively which expressed in Eq. (1).

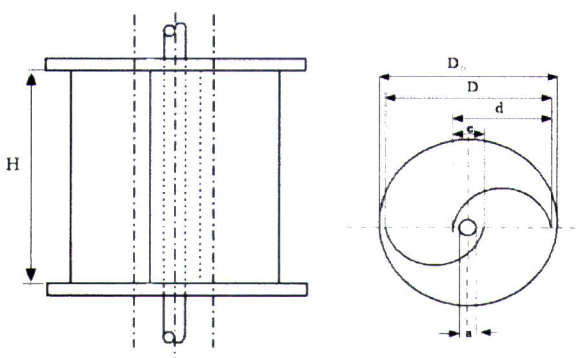


**Fig. 3.** Schematic diagram of Savonius rotor wind turbine [15]

$$A_s = H \times D \tag{1}$$

### *2.1.2 Mechanical Power ($P_m$)*

The mathematical representation of the energy generation process involves the concept of mechanical power ($P_m$). In this context, mechanical power is defined as the product of torque ($T$) and angular velocity ($\omega$), as expressed in Eq. (2).

$$P_m = T \times \omega \tag{2}$$

To calculate the mechanical power ($P_m$) of the mixed VAWT, it essential to determine the value of the torque. Torque ($T$) of the mixed VAWT is determined by multiplication of moment of inertia ($I$) and rotor angular acceleration ($\alpha$), as expressed in Eq. (3).

$$T = I \times \alpha \tag{3}$$

The mass of Savonius blade ($m$) is necessary to calculate the total rotor moment of inertia ($I_T$). In this study two distinct moments of inertia have been determined and expressed in Eq. (4) and Eq. (5): the moment of inertia of Savonius blade ($I_B$) and the moment of inertia of shaft ($I_S$).

$$I_B = m \times r^2 \times \frac{8}{3\pi} \tag{4}$$

$$I_S = \frac{m}{12} \times L^2 \tag{5}$$

$$I_T = I_B + I_S \tag{6}$$

where $r$ is the radius and $L$ is the shaft length. Next, the calculation of angular acceleration ($a$) is expressed in Eq. (7), where $\omega_2$ and $\omega_1$ represent the final and initial angular velocities, respectively and $t$ denotes the time interval.

$$a = \frac{\omega_2 - \omega_1}{t} \tag{7}$$

*2.1.3 Power Coefficient ($C_p$)*

The efficiency of mixed VAWT is measured by the power coefficient ($C_p$), which is the ratio of the mechanical power (output power) to the total power available in the wind (input power). By utilising the Eq. (8), the power Coefficient ($C_p$) can be determined as:

$$C_p = \frac{\text{Mechanical power}}{\text{Power available in wind}} = \frac{P_m}{P_a} = \frac{\mathrm{T} \times \omega}{\frac{1}{2} \times \rho \times \mathrm{H} \times \mathrm{D} \times U^3} \tag{8}$$

where ρ is the density of air and $U$ is the wind speed.

*2.1.4 Tip Speed Ratio (λ)*

The tip speed ratio (λ) is the most commonly and conveniently used scaling parameter, integrating the principal aerodynamic effects of wind speed, rotor size and angular speed. It is calculated as the product of the ratio of the blade radius ($R$) to the angular speed of the rotor ($\omega$) and the velocity of the wind ($V_{rotor}$). The tip speed ratio can be defined using the dimensional state expressed in Eq. (9) and shown in Figure 4.

$$\lambda = \frac{V_{rotor}}{\omega R} \tag{9}$$

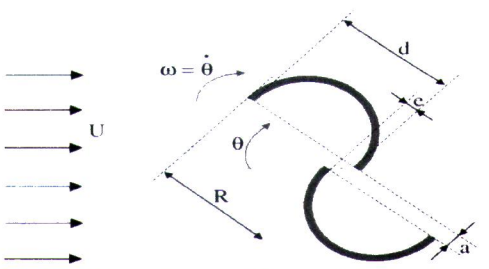


**Fig. 4.** Scheme of Savonius VAWT showing the tip velocity [15]

### *2.2 Mixed VAWT blade design*

A model of a mixed VAWT was designed and fabricated within the margin limitation of the wind tunnel test section at UPNM lab facilities, limited to dimensions of 30 cm x 30 cm x 100 cm, as depicted in Figure 6 below. The baseline design of the mixed VAWT was initially designed using SolidWorks software, followed by fabrication through a 3D printer. For this study, two blades of Savonius with a height of 11 cm, an overlap ratio of 0.08 and a plate thickness of 0.50 cm was considered as a baseline design. These Savonius blades were secured with endplates, one with a diameter of 14 cm and the other with a diameter of 15.5 cm, constructed from Polylactic Acid (PLA). The choice of PLA, a high-quality material known for its reliability and ease of printing, was deemed suitable for applications with flat surfaces, hard angles, or those requiring tight tolerances.

Additionally, Darrieus wind turbines were incorporated into the study, each featuring three blades with a height of 24 cm and a blade chord of 5 cm. The chosen blade airfoil type for the Darrieus wind turbine was DUW 200. Figure 5 presents a parametric study encompassing six designs of the mixed VAWT, showcasing variations in the arrangement of Savonius blade stages, blade diameter and the blade angle of the Darrieus component. This configuration results in six distinct models, each differing in diameter, stage type and angle of attack (AoA). The Figure 5 illustrates the dimensional specifications of each model and Table 2 provides a detailed tabulation of the design particulars. Furthermore, Figure 6 offers a comprehensive view of the assembled baseline design of the mixed VAWT.

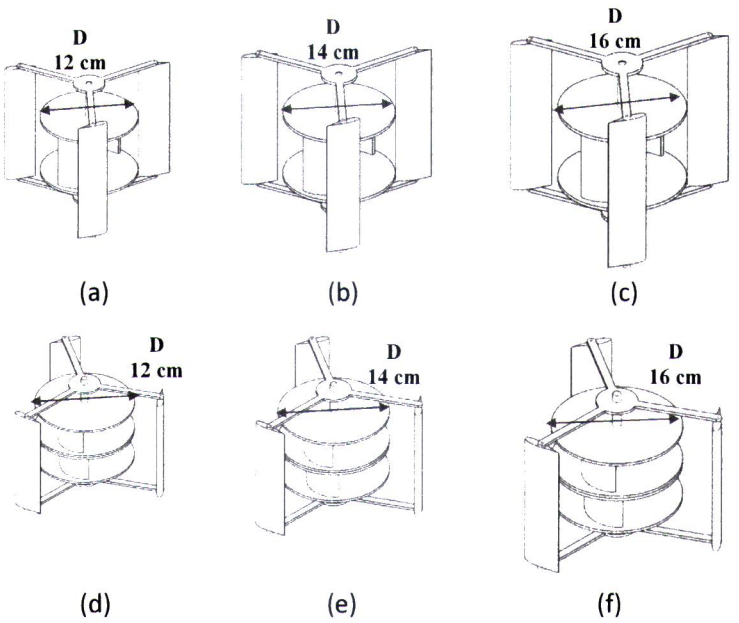


**Fig. 5.** Parameter specification design of mixed VAWT

**Table 2**
Parameter specification design of mixed VAWT

| Blade design | Blade diameter (cm) | Stages of the blade | Blade angle (°) |
|---|---|---|---|
| (a) | 12 | Single | 5 and 7 |
| (b) | 14 | Single | 5 and 7 |
| (c) | 16 | Single | 5 and 7 |
| (d) | 12 | Double | 5 and 7 |
| (e) | 14 | Double | 5 and 7 |
| (f) | 16 | Double | 5 and 7 |

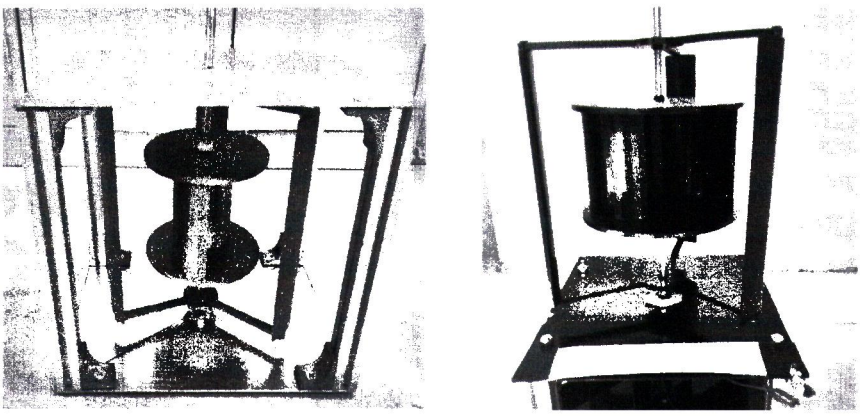

(a) Model for wind tunnel test (b) Small-scale mixed VAWT

**Fig. 6.** Complete assembling a model of MAWT

### *2.3 Experimental Setup*

The mixed VAWT model was accurately installed in the wind tunnel's test section. It was positioned under fixed conditions and oriented to face the wind direction to ensure accuracy and avoid errors. Figure 7 illustrates the mixed VAWT model within the wind tunnel test section, both without a generator and with a generator

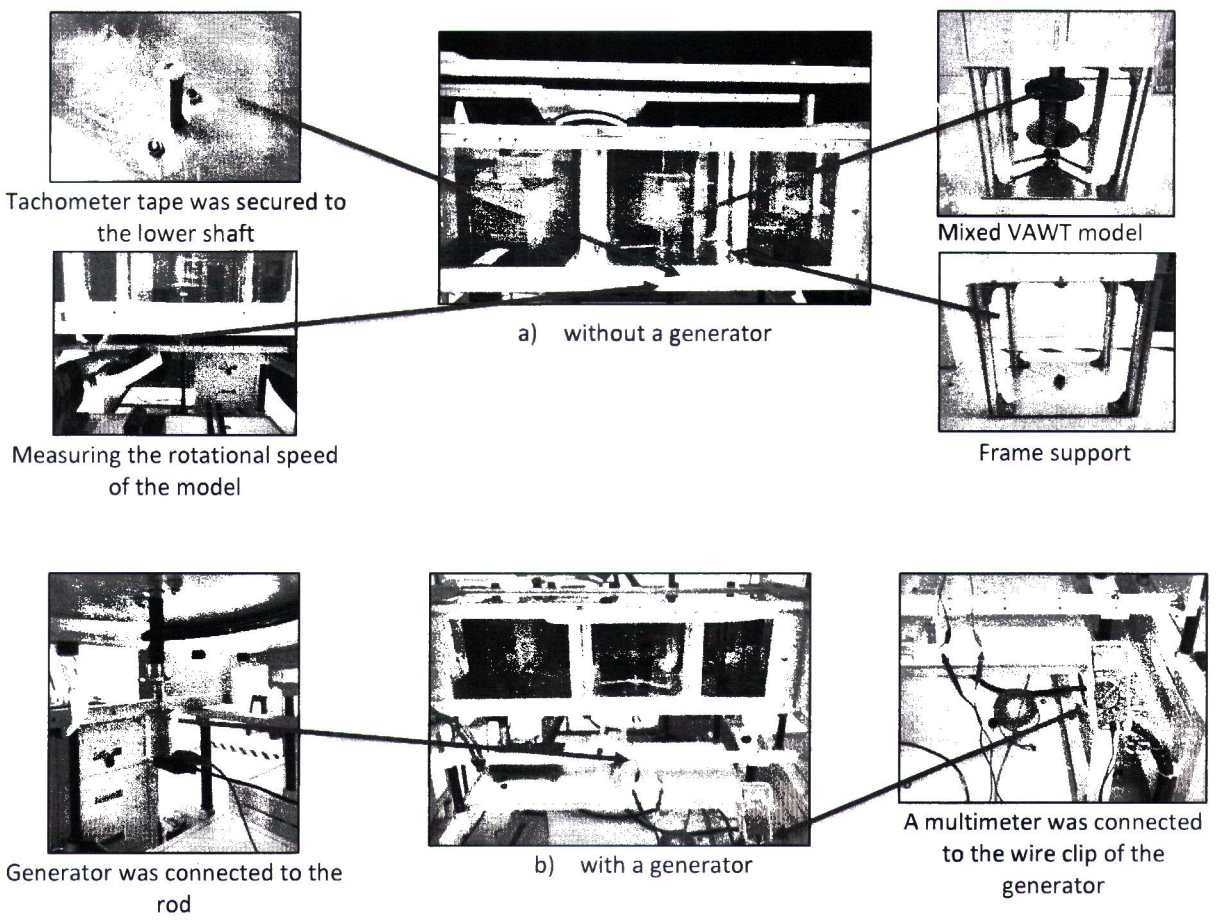


**Fig. 7.** Mixed VAWT model inside the wind tunnel test section

The wind turbine's blades were attached using a 10 mm diameter steel rod, serving as the mixed VAWT's shaft. This steel rod was connected to the upper and lower bases of the aluminum frame and positioned within the wind tunnel for testing. Wind tunnel velocities ranged from 0 to 9 m/s and data were collected using a digital laser tachometer while the shaft rotated to determine revolutions per minute (RPM). The tachometer was employed to ascertain the angular speed of the rotating shaft by converting its readings to RPM. The non-contact tachometer model used in this experiment featured reflective tape secured to the lower shaft for the tachometer's laser readings. According to Taguchi's experimental design proposal, orthogonal arrays are used to organise the parameters impacting the process and the levels at which should be varied. Similar to factorial design, the Taguchi approach tests combinations rather than all possible combinations, as factorial design does. This experiment involved three factors, each with three levels. The Taguchi L36 ($3^1$ X $2^2$) orthogonal array was selected before the wind tunnel test, resulting in 36 runs based on the Taguchi method's L36 orthogonal array. The chosen factors for this study include blade diameter, blade stages and angle of attack, each with three levels. Table 3 outlines the parameters used in optimising the mixed VAWT, representing a combination of multiple factors at various levels. Each design parameter consists of three-level criteria to enhance the performance of the mixed VAWT

**Table 3**
Factor of optimisation

| Factor | Design Parameters | Level 1 | Level 2 | Level 3 |
|---|---|---|---|---|
| A | Blade stages | single | double | - |
| B | Blade angle | 5 | 7 | - |
| C | Savonius blade diameter (cm) | 12 | 14 | 16 |

## 3. Results

### *3.1 Wind Feasibility Analysis*

The wind speed study was conducted as a pivotal parameter analysis to define the wind speed range in the wind tunnel. Concurrently, a wind feasibility study was undertaken in the Malaysian region to identify the optimal design for the mixed VAWT model, specifically tailored for potential offshore locations characterised by low wind speed conditions. Figure 8 illustrates the graph detailing daily wind speed and average electricity production across nine (9) selected offshore locations in Malaysia, with data collected and extracted using Renewable Ninja Tools. Significantly, the Mersing area exhibited the highest values for both average daily wind speed of 4.26 m/s and average electricity production is 0.0823 kW. This underscores the pivotal influence of wind turbine elevation on wind flow and electricity generation, given Mersing's setup at the elevated altitude of 43.6 meters. Consequently, the consistent elevation advantage renders the wind flow in the Mersing Area perpetually higher compared to other locations. Further analysis of the results reveals the average wind speeds extracted from various offshore locations: 2.61 m/s in Kuala Terengganu, 4.26 m/s in Mersing, 3.49 m/s in Pulau Langkawi, 2.26 m/s in Kota Kinabalu, 1.02 m/s in Sandakan, 2.31 m/s in Tawau, 2.1 m/s in Kudat, 1.07 m/s in Bintulu and 0.98 m/s in Kuching.

These findings collectively establish the average wind speed in the Malaysian region at 2.19 m/s, indicative of a low wind speed condition range. The observed data highlights the potential influence of factors such as elevation, geographical area and monsoon season on wind speed dynamics. Consequently, based on the comprehensive average wind speed data collected, the wind speed range chosen for this study extends up to a maximum speed of 9 m/s. This approach ensures an in-depth exploration of wind dynamics in Malaysia, laying the groundwork for subsequent wind tunnel tests and system optimisations.

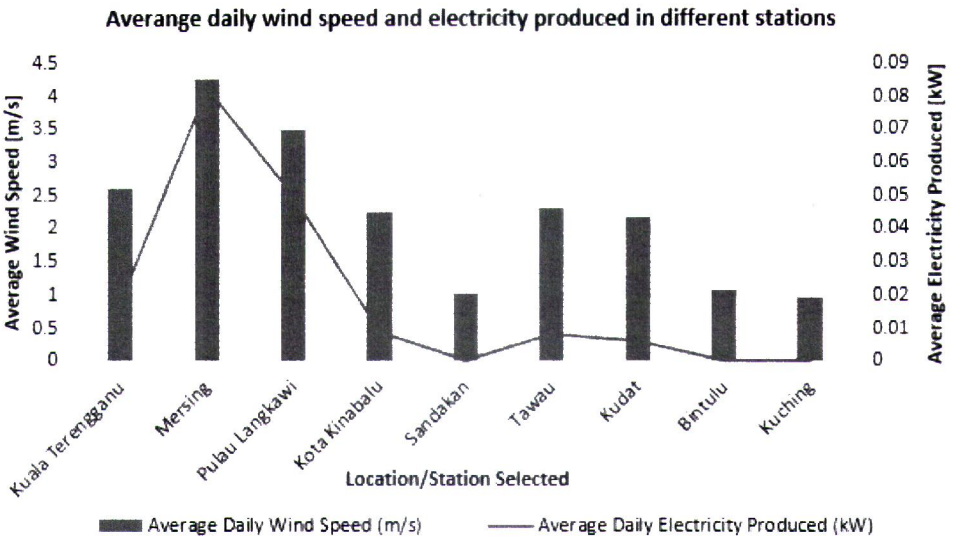


**Fig. 8.** Average Daily Wind Speed and Electricity Produced in nine (9) potential offshore in Malaysia

### *3.1 Diameter of blades*

The initial step in optimisation involved a comparison of the performance of wind turbines with different blade diameters (12 cm, 14 cm and 16 cm), focusing on the power coefficient ($C_p$) produced. These diameters were paired with both single and double stages of Savonius blades. The Savonius blade's diameter proved influential in determining the overall performance of the wind turbine. Table 4 presents the variation of power coefficient ($C_p$) across wind speeds ranging from 5 m/s to 9 m/s for the different diameters.

In comparison to smaller diameters, the power coefficient ($C_p$) for larger diameters increased from 0.539 to 0.622 for double stages and single stage, respectively. The data also revealed an upward trend in power as the number of blade stages increased, particularly for a 16 cm diameter blade. Subsequently, the power coefficient ($C_p$) was observed to be highest at a diameter of 16 cm for both single and double stages when considering all models with different diameters. The wind concentration on the blade was found to be less with single and double stages of smaller diameters. Consequently, a design with a 16 cm diameter, showcasing the highest power coefficient ($C_p$), was selected for further optimisation with other parameters, including blade stages and attack angles, as depicted in Figures 9 and 10.

**Table 4**
Power coefficient produced by each design at AoA 7°

| Diameter, cm | Power Coefficient ($C_p$) | |
|---|---|---|
| | Single | Double |
| 12 | 0.508 | 0.489 |
| 14 | 0.334 | 0.364 |
| 16 | 0.622 | 0.539 |

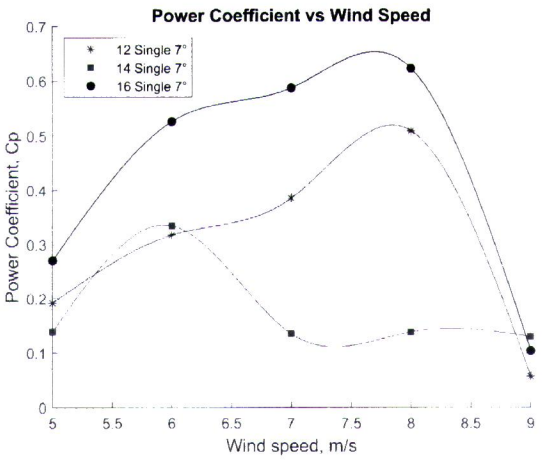


**Fig. 9.** $C_p$ against wind speed (single stage with at AoA 7°)

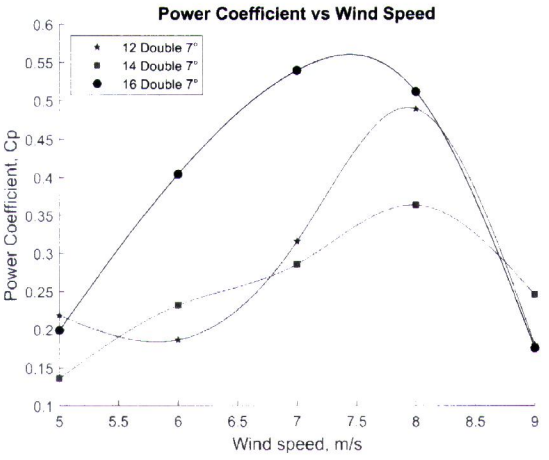


**Fig. 10.** $C_p$ against wind speed (double stages with at AoA 7°)

### *3.2 Different stages of the blade*

The second step in the optimisation process involved a comparison between the performance of single and double stages of the wind turbine. The analysis focused on the variation of stages using 16 cm diameter blades, providing a detailed examination of the power coefficient ($C_p$) to better understand the performance of the wind turbine blades. Figure 11 illustrates that single-stage wind turbines outperform their double-stage counterparts, showing higher efficiency. Both designs exhibit an increasing trend, reaching a peak at a wind speed of 8 m/s. The power coefficient ($C_p$) was closely observed during the transition from a single stage to a double stages. Experimental results presented in Table 5 indicated that the single stage model achieved the highest power coefficient ($C_p$). Specifically, at an AoA 5° and AoA 7°, the power coefficients ($C_p$) for the single stage were 0.678 and 0.622, respectively. In contrast, the double stage exhibited power coefficients of 0.448 and 0.539 at a wind velocity of 8 m/s. Figures 11 and 12 further illustrates the graph patterns of both models at different angles of attack, indicating that both stages reach their maximum rotation speed from 236 RPM to 310 RPM at a wind speed of 8 m/s. Notably, nearly all power coefficients ($C_p$) values peaked at a wind speed of 8 m/s for a 16 cm diameter.

For double stages, at an AoA 7°, the power coefficient power coefficients ($C_p$) peaked at 7 m/s but dropped to 0.180. Irrespective of the angle of attack, the single stage consistently exhibited a higher power coefficient ($C_p$) than the double stages. Additionally, at a wind speed of 9 m/s, the single stage rotated more slowly than the double stages for both angles AoA, as depicted in Figure 11 and Figure 12. This discrepancy was attributed to reaching the RPM and power limits, impacting energy efficiency. The use of a single stage significantly contributed to balancing variations in generated torque, resulting in positive values at all rotor angles. This improvement enhances the Savonius rotor's self-starting ability and overall performance. Furthermore, single stage provides a larger surface area to capture more wind flow compared to double stages. In summary, the second step of the optimisation demonstrated that the single stage design yielded the best performance, producing the highest power coefficient ($C_p$).

**Table 5**
Power coefficient ($C_p$) produced by each design at 16 cm diameter

| Stages | single | | double | |
|---|---|---|---|---|
| Angle of attack | 5˚ | 7˚ | 5˚ | 7˚ |
| Power Coefficient ($C_p$) | 0.678 | 0.622 | 0.448 | 0.539 |

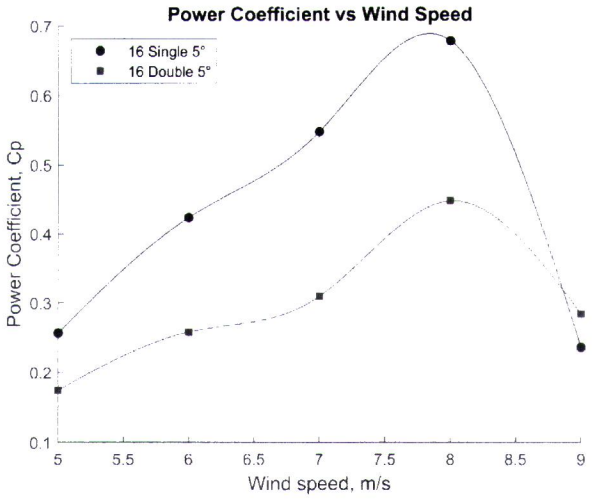


**Fig. 11.** $C_p$ against wind speed of AoA of 5˚

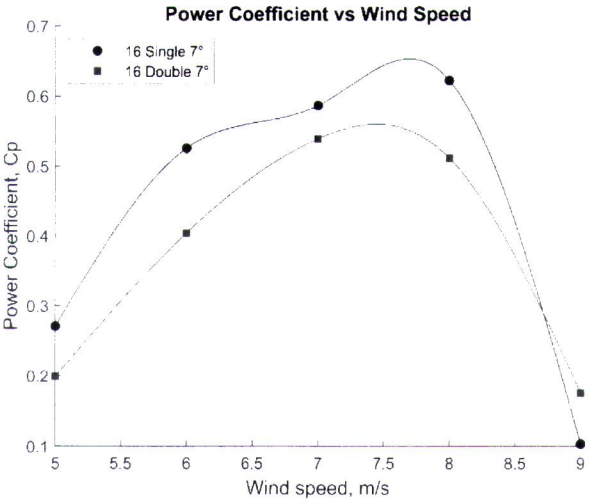


**Fig. 12.** $C_p$ against wind speed of AoA of 7˚

### *3.3 Different angles of attack of the blades*

The third optimisation step involved a comparative analysis of the wind turbine's performance with varying angles of attack (AoA), measured in terms of the power coefficient ($C_p$). These angles were combined with 16 cm diameter single stage blade for the Savonius blade. The angle of attack is a crucial parameter known to influence rotation, particularly in three-dimensional aerodynamic models of rotating wind turbines. As presented in Table 6, the highest efficiency performance was achieved with a turbine set at an AoA 5˚. However, at an AoA 7˚, the angle surpassed the critical threshold, resulting in decreased efficiency. From Figure 13, the power coefficient ($C_p$) ranged from a minimum of 0.236 to a maximum of 0.678 for the two variations in angle. Notably, the AoA 5˚ yielded the highest power coefficient ($C_p$) with a turbine rotation speed of 307 RPM, while AoA 7˚ resulted in a speed of 313 RPM. These findings indicate that the turbine set at an AoA 5˚ can operate more optimally than the AoA 7˚. However, it's worth noting that two instances of the highest power coefficient ($C_p$) values were achieved at AoA 7˚ compared to AoA 5˚. Consequently, it can be concluded that the AoA 7˚ is the optimal angle of attack for the Darrieus blade in a mixed VAWT under low wind speed conditions.

**Table 6**
Power coefficient ($C_p$) produced by 16 cm of single stages (AoA 5˚ and AoA 7 ˚)

| Angle of attack | 5 ˚ | 7 ˚ |
|---|---|---|
| Power Coefficient ($C_p$) | 0.678 | 0.622 |

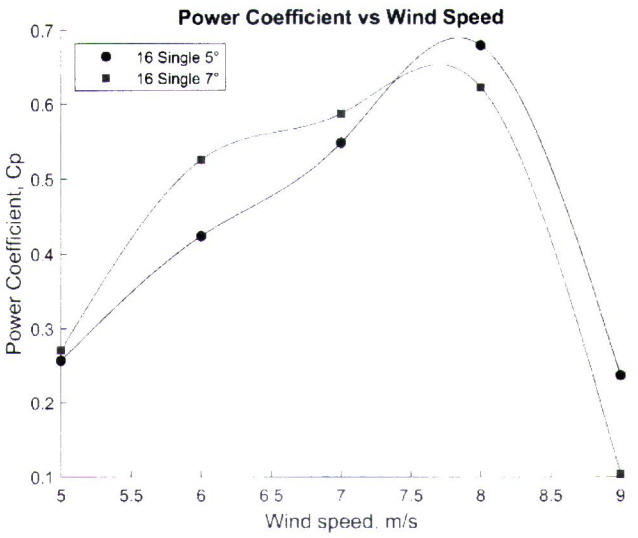


**Fig. 13.** Power coefficient ($C_p$)against wind speed of 16 cm for single stage at AoA 5°and AoA 7°

### 3.5 *Result of Taguchi design analysis*

The present study demonstrates the application of the Taguchi method for optimising blade performance characteristics of a mixed VAWT, employing the calculation of power coefficients to establish design parameters efficiently. Figure 14 (a) presents an overview of the mean Signal-to-Noise Ratio (MSNR) profile for the three different factors considered in this study. The method showcases combinations of designed experiments using an orthogonal array. Table 7 highlights the highest Signal-to-Noise Ratio (SNR) values, with a peak of -4.958 at level 3 for the diameter factor. The delta represents the difference between the highest and lowest average response values for each factor. In comparison to the other two factors, the diameter factor exhibits the greatest difference in the response table of SNR and means, with values of 4.218 and 0.2075, respectively, followed by stages and angle of attack. This substantial increase in MSNR appears to significantly enhance the efficiency of the turbine system.

The effect of each factor can be computed by subtracting the lowest from the highest mean SNR ratios. A larger difference indicates a greater effect value of the factor, representing a substantial function in the wind turbine system's performance. As mentioned earlier, a larger SNR ratio corresponds to a higher power coefficient ($C_p$). Figure 14 (b) clearly illustrates that a combination of a 16 cm diameter with single stage and an AoA 7° is the optimum level for a wind turbine, as the mean SNR ratio is largest at this level. Larger factor effects correspond to greater influence on the power coefficient ($C_p$). The effect of 0.5719 has the most impact on wind turbine performance, while 0.3644 has the least effect. These findings indicate that the optimal design can effectively increase the output power performance of VAWT systems. The study's results identify the most optimal power condition as a diameter of 16 cm, single stage and an AoA 7°. Diameter is deemed the most significant influencing factor based on Taguchi analysis, ranked 1$^{st}$ in the Signal-to-Noise ratio analysis, followed by single stages in 2$^{nd}$ place and angle of attack in 3$^{rd}$ place. The higher the diameter, the greater the generated rotor power. Ranks in the response table help identify factors with the largest effects, with rank 1 assigned to the factor with the largest delta value, rank 2 to the second largest and rank 3 to the third largest.

**Table 7**
Response table for signal-to-noise ratios (SNR)

| Level | Diameter (12 cm 14 cm & 16 cm) | Stages (Single & Double) | Angle of attack (5 ° & 7 °) |
|---|---|---|---|
| 1 | -7.255 | -6.916 | -7.613 |
| 2 | -9.177 | -7.344 | -6.647 |
| 3 | -4.958 | - | - |
| Delta | 4.218 | 0.428 | 0.966 |
| Rank | 1 | 2 | 3 |

**Table 8**
Response table for means

| Level | Diameter (12 cm 14 cm & 16 cm) | Stages (Single & Double) | Angle of attack (5 °& 7 °) |
|---|---|---|---|
| 1 | 0.4663 | 0.4829 | 0.4590 |
| 2 | 0.3644 | 0.4522 | 0.4761 |
| 3 | 0.5719 | - | - |
| Delta | 0.2075 | 0.0306 | 0.0171 |
| Rank | 1 | 2 | 3 |

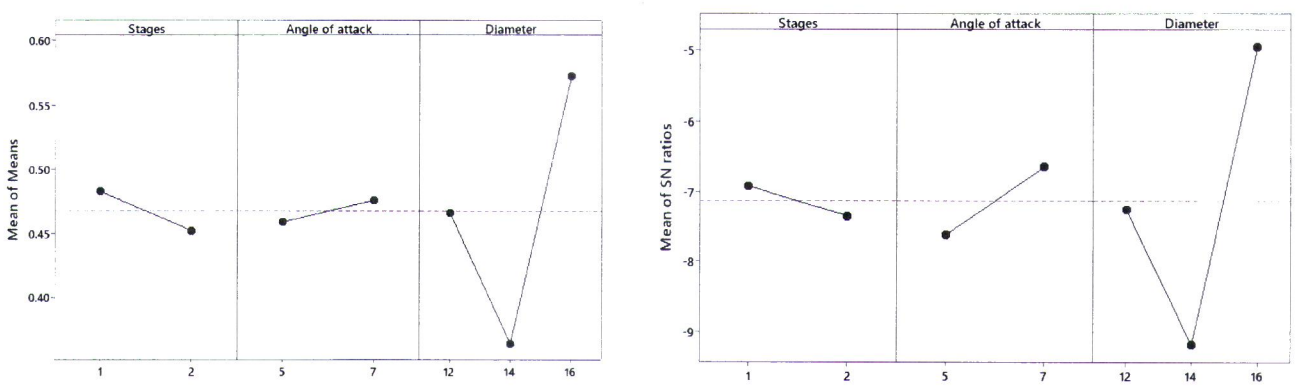


(a) (b)

**Fig. 14** Main effects plot for (a) means and (b) SNR values

## 4. Conclusions

In summary, this study has effectively achieved its goal of optimising the mixed VAWT blade design for low wind speed conditions. The thorough optimisation process, considering parameters such as blade diameter, stage and angle of attack, produced promising outcomes. Through validated results obtained from wind tunnel tests, it was demonstrated that the combination of a 16 cm diameter, single stage, with an AoA 7° stands out as the most effective design under low wind speed conditions. Furthermore, the study conducted a comprehensive evaluation of wind turbine blade performance, specifically focusing on the power coefficient ($C_p$). The findings underscored the significant influence of manipulating different parameters in Darrieus and Savonius blade designs on the overall performance of the wind turbine, demonstrated through variations in the power coefficient ($C_p$). In conclusion, the successful optimisation and performance evaluation conducted in this study not only provide valuable insights into enhancing mixed VAWT blade design but also emphasise the importance of considering diverse parameters to achieve optimal performance in low wind speed conditions. These results offer a solid foundation for further advancements in VAWT technology, with potential applications in regions characterised by lower wind speeds.

## Acknowledgement
This research was not funded by any grant.

## References
[1] Khillar, S. "Difference between horizontal and vertical axis wind turbine." October 17, 2019. http://www.differencebetween.net/technology/difference-between-horizontal-and-vertical-axis-wind-turbine/
[2] Johari, M. Khudri, Muhd Jalil, and Mohammad Faizal Mohd Shariff. "Comparison of horizontal axis wind turbine (HAWT) and vertical axis wind turbine (VAWT)." *International Journal of Engineering and Technology* 7, no. 4.13 (2018): 74-80. https://doi.org/10.14419/ijet.v7i4.13.21333
[3] Óskarsdóttir, M.Ó. "A general description and comparison of horizontal axis wind turbines and vertical axis wind turbines. " Master's thesis, Faculty of Industrial Engineering & Mechanical Engineering, University of Iceland, 2014. https://skemman.is/bitstream/1946/19859/1/Margr%C3%A9t%20%C3%93sk%20%C3%93skarsd%C3%B3ttir.pdf
[4] Jamanun, M. J., Misaran M. S., Rahman M., and Muzammil W. K. "Performance investigation of a mix wind turbine using a clutch mechanism at low wind speed condition." In *IOP Conference Series: Materials Science and Engineering*, vol. 217, no. 1, p. 012020. IOP Publishing, 2017. https://doi.org/10.1088/1757-899x/217/1/012020
[5] Mekhilef, Saad, and Chandrasegaran D. "Assessment of off-shore wind farms in Malaysia." In TENCON 2011-2011 IEEE Region 10 Conference, pp. 1351-1355. IEEE, 2011. https://doi.org/10.1109/tencon.2011.6129028
[6] Albani, Aliashim, and Ibrahim M.Z. "Wind energy potential and power law indexes assessment for selected near-coastal sites in Malaysia." *Energies* 10, no. 3 (2017): 307. https://doi.org/10.3390/en10030307
[7] Hashim, F. E, Peyre, O., Lapok S. J., Yaakob O., and Din A. H. M. "Offshore wind energy resource assessment in Malaysia with satellite altimetry." Journal of Sustainability Science and Management 15, no. 6 (2020): 111-124. https://doi.org/10.46754/jbsd.2020.08.010
[8] Azmi. "Wind energy landscape in Malaysia" May 21, 2020. https://www.azmilaw.com/insights/wind-energy-landscape-in-malaysia/
[9] Albani, Aliashim, and Ibrahim M.Z. "Statistical analysis of wind power density based on the Weibull and Rayleigh models of selected site in Malaysia." Pakistan Journal of Statistics and Operation Research (2013): 395-408. https://doi.org/10.18187/pjsor.v9i4.580
[10] Ho, L. W. "Wind energy in Malaysia: past, present and future." *Renewable and Sustainable Energy Reviews* 53 (2016): 279-295. https://doi.org/10.1016/j.rser.2015.08.054
[11] Chiang, E. P., Z. A. Zainal, Aswatha N., and Seetharamu K. N. "The potential of wave and offshore wind energy in around the coastline of Malaysia that face the South China Sea." (2006)
[12] Abdullah, Wan S. W, Osman M., Kadir M.Z.A, and Verayiah R. "The potential and status of renewable energy development in Malaysia." Energies 12, no. 12 (2019): 2437. https://doi.org/10.3390/en12122437
[13] Sharuddin, Syahidah N., Ng C. H., Tuhaijan S. N. A, Kurian V. J., and Wong L. W. "An evaluation of offshore wind renewable energy performance in Malaysia." International Journal of Biomass and Renewables 8, no. 1 (2019): 25-33.
[14] Mahmoud, N. H., El-Haroun A. A., Wahba E., and Nasef M. H. "An experimental study on improvement of Savonius rotor performance." Alexandria Engineering Journal 51, no. 1 (2012): 19-25. https://doi.org/10.1016/j.aej.2012.07.003
[15] Menet, Jean-Luc, and Bourabaa N. "Increase in the Savonius rotors efficiency via a parametric investigation." In European Wind Energy conference & exhibition, pp. 22-25. 2004.
[16] Osmi S. K. C, Rosdi A., Husen H., Sojipto S., Misnon N. A., and Khairuddin F.H. "Numerical simulation and full-scale field testing of steel parapet railing under impact of heavy truck loads–comparative study." In IOP Conference Series: Earth and Environmental Science, vol. 476, no. 1, p. 012056. IOP Publishing, 2020. https://doi.org/10.1088/1755-1315/476/1/012056
[17] Nordin N., Nadzri M. N. A, Bohari B., Saad M. R, and Othman M. "Experimental Investigation of Savonius Wind Turbine Blade For Low Wind Speed Region." Zulfaqar Journal of Defence Science, Engineering & Technology 5, no. 1 (2022).
[18] Maidiana O., Frost M., and Dixon N. "Stability performance and interface shear strength of geocomposite drain/soil systems." In AIP Conference Proceedings, vol. 1930, no. 1. AIP Publishing, 2018. https://doi.org/10.1063/1.5022943
[19] Nordin N., Bohari B., Chandrasegaran T., As'array. A, and Harmin M. Y. "Load Case Selection Technique for Combined Modal Finite Element Approach of High Aspect Ratio Wing Models." Journal of Aeronautics, Astronautics and Aviation 55, no. 3S (2023): 425-437. https://doi.org/10.6125/JoAAA.202309_55(3S).02
[20] Sidik, N. A. C, Musa S., Yusof S. N. A, and Ediwansyah E. "Analysis of Internal Flow in Bag Filter by Different Inlet Angle." Journal of Advanced Research in Numerical Heat Transfer 3, no. 1 (2020): 12-24.

[21] Mohamad, Tajuddin A., Kaur J., Sidik N. A. C., and Rahman S. "Nanoparticles: A review on their synthesis, characterization and physicochemical properties for energy technology industry." Journal of Advanced Research in Fluid Mechanics and Thermal Sciences 46, no. 1 (2018): 1-10.

[22] Al-Ghriybah, Mohanad, Zulkafli M.F, and Djamal H. Didane. "Numerical investigation of inner blade effects on the conventional savonius rotor with external overlap." Journal of Sustainable Development of Energy, Water and Environment Systems 8, no. 3 (2020): 561-576. https://doi.org/10.13044/j.sdewes.d7.0292

[23] Zemamou, M., Aggour M., and Toumi A. "Review of savonius wind turbine design and performance." Energy Procedia 141 (2017): 383-388. https://doi.org/10.1016/j.egypro.2017.11.047

[24] Loganathan, Bavin, Mustary I., Chowdhury H., and Alam F. "Effect of sizing of a Savonius type vertical axis micro wind turbine." Energy Procedia 110 (2017): 555-560. https://doi.org/10.1016/j.egypro.2017.03.184

[25] Kadam, A. A., and Patil S. S. "A review study on Savonius wind rotors for accessing the power performance." IOSR Journal of Mechanical and Civil Engineering 5 (2013): 18-24.

[26] Prince, Simon A., Badalamenti C., and Georgiev D. "Experimental investigation of a variable geometry vertical axis wind turbine."Wind Engineering 45, no. 4 (2021):904-920. https://doi.org/10.1177/0309524x20935134